frontiers in Earth Science

ORIGINAL RESEARCH
published: 26 May 2021
doi: 10.3389/feart.2021.644142

Focal Mechanism and Seismogenic Structure of the M_S 5.1 Qingbaijiang Earthquake on February 3, 2020, Southwestern China

Min Zhao, Feng Long, Guixi Yi, MingJian Liang, Jiangtao Xie and Siwei Wang*

Sichuan Earthquake Administration, Chengdu, China

The 3 February 2020 M_S 5.1 Qingbaijiang earthquake, southwestern China, is the closest recorded $M_S \geq 5.0$ event to downtown Chengdu City to date, with an epicentral distance of only 38 km. Here we analyze seismic data from the Sichuan and Chengdu regional seismic networks, and employ a multi-stage location method to relocate the earthquakes that have occurred along the central and northern segments of the Longquanshan fault zone since 2009, including the M_S 5.1 Qingbaijiang earthquake sequence, to investigate the seismogenic structure of the region. The relocation results indicate that the seismicity along the central and northern segments of the Longquanshan fault zone has occurred mainly along the eastern branch since 2009, with the hypocentral distribution along a vertical cross-section illustrating a steep, NW-dipping parallel imbricate structure. The terminating depth of the eastern branch is about 12 km. The distribution of the M_S 5.1 Qingbaijiang earthquake sequence is along the NE–SW-striking Longquanshan fault zone. The aftershock focal depths are in the 3–6 km range, with the mainshock located at 104.475°E, 30.73°N. Its initial rupture depth of 5.2 km indicates that the earthquake occurred above the shallow decollement layer of the upper crust in this region. The hypocentral distribution along the long axis of the aftershock area highlights that this earthquake sequence occurred along a fault dipping at 56° to the NW. Our surface projection of the inferred fault plane places it near the eastern branch of the Longquanshan fault zone. We infer the M_S 5.1 mainshock to be a thrust faulting event based on the focal mechanism solution via the cut-and-paste waveform inversion method, with strike/dip/rake parameters of 22°/36°/91° and 200°/54°/89° obtained for nodal planes I and II, respectively. We identify that the seismogenic fault of the M_S 5.1 Qingbaijiang earthquake lies along the eastern branch of the Longquanshan fault zone, and nodal plane II represents the coseismic rupture plane, based on a joint analysis of the event relocation results, mainshock focal mechanism, and regional geological information. Our study provides vital information for assessing the seismic hazard of the Longquanshan fault zone near Chengdu City.

Keywords: the MS 5.1 Qingbaijiang earthquake, relocation, focal mechanism solution, seismogenic structure, the Longquanshan fault zone

OPEN ACCESS

Edited by:
Ruizhi Wen,
Institute of Engineering Mechanics, China

Reviewed by:
Jorge Jara,
École Normale Supérieure, France
Dogan Kalafat,
Boğaziçi University, Turkey

****Correspondence:***
Guixi Yi
yigx64@163.com

Specialty section:
This article was submitted to Structural Geology and Tectonics, a section of the journal Frontiers in Earth Science

Received: *20 December 2020*
Accepted: *26 April 2021*
Published: *26 May 2021*

Citation:
Zhao M, Long F, Yi G, Liang M, Xie J and Wang S (2021) Focal Mechanism and Seismogenic Structure of the M_S 5.1 Qingbaijiang Earthquake on February 3, 2020, Southwestern China. Front. Earth Sci. 9:644142. doi: 10.3389/feart.2021.644142

INTRODUCTION

The ongoing Cenozoic collision between the Indian and Eurasian plates has contributed to the uplift of the Tibetan Plateau (Molnar and Tapponnier, 1975; Houseman and England, 1986; Yin and Harrison, 2000; Tapponnier et al., 2001). However, eastward growth of the Tibetan Plateau has been impeded by the tectonically stable Yangtze Block, with the Longmenshan fold-and-thrust belt (LFTB) and the associated uplift of the Sichuan foreland basin and Longquanshan anticline forming in the eastern part of the Tibetan Plateau (Tapponnier and Molnar, 1977; Tapponnier et al., 1982; Chen et al., 1994; Burchfiel et al., 1995; Chen and Wilson, 1996; Kirby et al., 2002). The LFTB is a geologically active area of the eastern Tibetan Plateau, as indicated by the 2008 M_S 8.0 Wenchuan and 2013 M_S 7.0 Lushan earthquakes (Burchfiel et al., 2008; Hubbard and Shaw, 2009; Xu et al., 2009, 2013; Yin, 2010). Numerous studies have focused on the Longmenshan fault zone following the 2008 Wenchuan earthquake (Kirby et al., 2008; Liu-Zeng et al., 2009; Li et al., 2010; Wang et al., 2010, 2011, 2012; Zhang et al., 2010; Zhang, 2013), and also the structural characteristics and seismic hazard along the range front of the LFTB (Parsons et al., 2008; Toda et al., 2008; Hubbard and Shaw, 2009; Liu-Zeng et al., 2009; Hubbard et al., 2010). The Longquanshan fault zone, which forms the southeastern boundary of the Sichuan basin (Deng et al., 1994), has been inferred to possess a low level of seismicity that is characterized by smaller-magnitude earthquakes (Li et al., 2015; Wang and Lin, 2017); consequently, its geometric structure and seismic hazard have not been well studied. The occurrence of the 3 February 2020 M_S 5.1 Qingbaijiang earthquake therefore provides an opportunity to study the structural characteristics and potential seismic hazard of the Longquanshan fault zone, since its epicenter and associated aftershocks have been located along the central and northern segments of the fault zone.

The M_S 5.1 Qingbaijiang earthquake occurred adjacent to the highly populated and economically developed Chengdu Plain. It is the closest $M_S \geq 5.0$ event to downtown Chengdu City to date, with an epicentral distance of only 38 km. Previous studies have considered the Sichuan Basin to be a stable terrane that poses no risk of strong earthquakes (Xu et al., 2006; Hubbard et al., 2010). However, recent studies have revealed that moderate-to-strong earthquakes may also occur along the Longquanshan fault zone (Li et al., 2012, 2013; Wang and Lin, 2017). Numerous concerns regarding the future seismic hazard of the Longquanshan fault zone have been raised following this event. However, the limited data means that more studies are needed to reassess the seismic hazard in the Longquanshan area.

Constraints on seismogenic structures and their associated earthquake mechanisms are helpful for seismic risk assessments. The characteristics of various geological structures can generally be recognized by the spatial distribution of relocated earthquakes (Michael, 1988; Shearer, 1997; Presti et al., 2008; Yi et al., 2015, 2017, 2019), and the geometric and kinematic characteristics of these seismogenic structures can be inferred from their associated earthquake focal mechanisms (Zheng et al., 2009; Lv et al., 2013; Yi et al., 2015, 2017, 2019, 2020). Here we analyze seismic phase and waveform data from the Sichuan and Chengdu seismic networks, and relocate the earthquakes that have occurred along the central and northern segments of the Longquanshan fault zone since 2009, which include the M_S 5.1 Qingbaijiang earthquake sequence. We then analyze the earthquake distribution along the central and northern segments of the Longquanshan fault zone and the seismogenic structure associated with the M_S 5.1 Qingbaijiang earthquake sequence. We confirm the structure via a joint analysis of the earthquake relocation results, mainshock focal mechanism solution, and existing regional geological data, and analyze the seismogenic mechanism. Our results are a first step in better understanding the seismogenesis of the Longquanshan fault zone, and provide essential data for future studies on the formation mechanism and seismic hazard of the fault zone.

GEOLOGICAL SETTING AND HISTORICAL EARTHQUAKES

The Longquanshan fault zone forms the eastern boundary of the western Sichuan foreland basin, extending along the eastern side of the Longmenshan thrust-nappe structure and the western front of the Sichuan Basin. This 200-km-long NE–SW-trending fault zone starts in Zhongjiang County at its northern end, transects Jintang and Renshou counties, and terminates near Xinqiao Town, Leshan County, at its southern end (Li and Zeng, 1994). The Longquanshan fault zone consists of eastern and western branches that are distributed along the eastern and western limbs of the Longquanshan anticline, respectively (**Figure 1**); a conceptual model of the fault zone is shown in **Figure 2**. The western branch generally strikes NE20°–NE30°, and consists of faults that dip to the SE at 35°–70° and form an imbricate nappe structure, with these faults converging along the same main reverse fault at depth, as inferred from geological mapping (**Figure 2**; Deng et al., 1994) and seismic profiling (Wang et al., 2008; Li et al., 2013). The eastern branch is nearly parallel to the western branch, with a strike of NE10°–NE30°, and it consists of faults that dip to the NW at 28°–82° (Huang and Tang, 1995; Huang and Jiang, 2012; Li et al., 2013). The primary strata of the Longquanshan anticline are Jurassic and Cretaceous in age (Deng et al., 1994), the Longquanshan fault zone extends through these Jurassic and Cretaceous strata and terminates in the Triassic strata (Huang and Tang, 1995). The Longquanshan fault zone is divided into northern, central, and southern segments, and previous studies have generally defined the western branch as the main fault of the fault zone (**Figure 1**; Deng et al., 1994; Huang and Tang, 1995; Wang et al., 2008). The Longquanshan fault zone was originally activated during the formation of the Tibetan Plateau at the end of the Eocene (Deng et al., 1994), as inferred from seismological and geological investigations, geodetic deformation surveys (Huang and Tang, 1995; Zhang et al., 2003; Burchfiel, 2004), and focal mechanism solutions (Cheng, 1981). The secondary western Sichuan Block within the Tibetan Plateau continued to move to the SE and collided with the South China Block, resulting in the formation of small-scale folds in the interior of the Sichuan Basin (Deng et al., 1994).

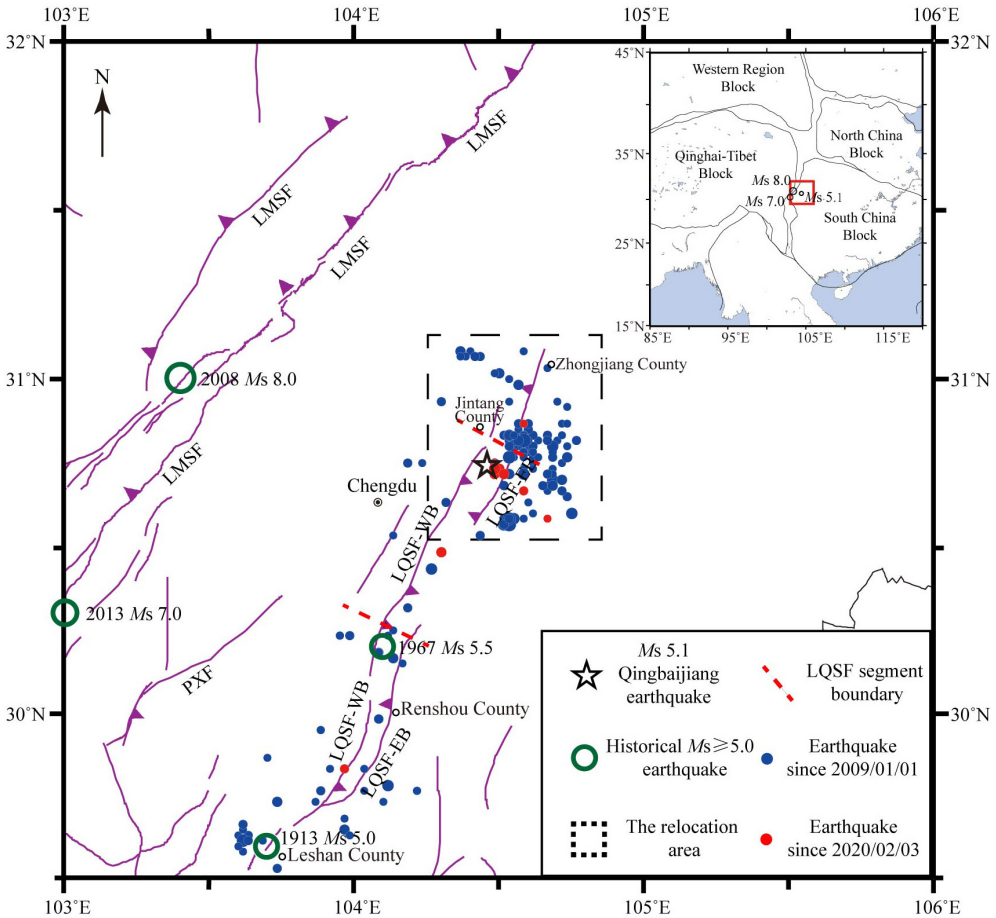

FIGURE 1 | Geological setting and epicentral map of $M_L \geq 2.0$ earthquakes since 2009 near the epicenter of the 3 February 2020 M_S 5.1 Qingbaijiang earthquake. Inset map in the upper right corner highlights the study area (red rectangle) in the main figure relative to the major crustal blocks in China. Purple lines indicate active faults: LMSF, Longmenshan fault zone; LQSF, Longquanshan fault zone; LQSF-EB, Eastern Branch of the Longquanshan fault zone; LQSF-WB, Western Branch of the Longquanshan fault zone; PXF, Pujiang-Xinjin fault.

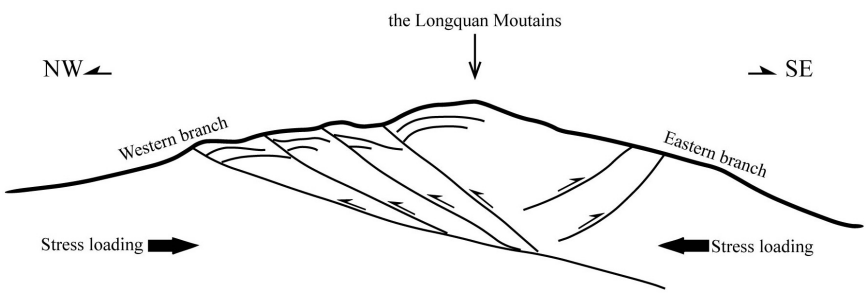

FIGURE 2 | Conceptual structural model of the Longquanshan fault zone (revised from Deng et al., 1994). The western branch consists of SE-dipping faults that form an imbricate nappe structure, with these faults converging along the same main reverse fault at depth. The eastern branch consists of NW-dipping faults with a nearly parallel arrangement.

The Longquanshan fault zone is a seismic zone that has generally hosted moderate-to-weak earthquakes, with segmented seismicity across the fault zone. Only two recorded $M_S \geq 5.0$ earthquakes have occurred along the southern segment of the fault zone (**Figure 1**), including the destructive 24 January 1967 M_S 5.5 Renshou earthquake, which is the largest event along the fault zone to date; this event had a 4 km focal depth and epicenter located on the southeastern side of the western branch (Cheng, 1981; Xu et al., 2006). Fault gouge dating has revealed that the Longquanshan fault zone was active

during the early to late Pleistocene, with the mid-Pleistocene being the most active period (Huang and Tang, 1995). Late Pleistocene activity was limited to the southern and central segments of the western branch, which might explain why moderate earthquakes have frequently occurred along these segments (Huang and Tang, 1995).

RELOCATION OF THE M_S 5.1 QINGBAIJIANG EARTHQUAKE SEQUENCE

Seismic Data and Relocation Method

The seismic phase data used for the earthquake relocation are from the Sichuan (black triangles in **Figure 3**) and Chengdu (green triangles in **Figure 3**) regional seismic networks. The M_S 5.1 Qingbaijiang earthquake sequence occurred in an area with dense, distributed seismic station coverage, thereby providing reliable data for our study. There were 55 broadband seismic stations within a 300 km epicentral distance of the mainshock, with an additional two portable short-period (SP) seismometers deployed near the epicenter immediately after the mainshock (red triangles in **Figure 3**). The minimum magnitude of completeness for the M_S 5.1 earthquake sequence was estimated to be 1.4 by the goodness-of-fit test (Wiemer and Wyss, 2000).

The events in the study area since the M_S 5.1 mainshock have been highly concentrated near the mainshock. We selected the events with epicentral distances within 15 km of the mainshock as aftershocks. The aftershocks of the M_S 5.1 event were sparse, with a scattered distribution of only 75 $M_L \geq 0.1$ aftershocks recorded by the end of October 2020 (**Figure 4**). The magnitude–time (M–t) plot (**Figure 4A**) shows that the aftershocks of the M_S 5.1 event occurred mainly during the first 2 months, whereas the aftershocks after 1 April 2020 were scattered. The frequency–time (N–t) plot (**Figure 4B**) shows that the monthly aftershock frequency of the sequence has been very low since April 2020, which indicates a rapid decay in the aftershock frequency.

We collected the phase data for 281 earthquakes since 2009 along the central and northern segments of the Longquanshan fault zone to obtain the necessary number of earthquakes for relative locations, and analyzed both the temporal and spatial characteristics of the seismicity along these segments. We relocated these earthquakes using the multi-stage method developed by Long et al. (2015). The details of our procedure are as follows.

We first located the initial earthquake locations using HYPOINVERSE2000 (Klein, 1989) based on the eastern Sichuan velocity model (Zhao and Zhang, 1987). We then selected the events that were recorded at six or more seismic stations and possessed a station distribution with a maximum azimuth gap of less than 180°. The lower limit number of observed stations in our study region was set to six, based on a series of test results, whereby the location accuracy was heavily reduced for fewer stations and the amount of relocated events decreased significantly with higher station limits, both of which inhibited the ability to accurately determine the geometry of the seismogenic fault. We calculated a new local one-dimensional (1-D) velocity model (**Table 1**) and station corrections via the VELEST program (Kissling et al., 1994, 1995) prior to the event relocations. We then employed hypoDD (Waldhauser and Ellsworth, 2000) to relocate the events using this new velocity model and applying the station corrections. We set a 3 km search radius to identify any earthquake clusters, since there were no tight earthquake distributions in the study area.

We relocated 199 earthquakes, including 60 events that were associated with the M_S 5.1 Qingbaijiang earthquake sequence. The average errors in the horizontal and vertical directions were 0.6 and 0.8 km, respectively, and the travel time residual was 0.2 s. The mainshock was located at 104.475°E, 30.731°N, with a focal depth of 5.2 km.

Analysis of the Relocation Results

The dashed rectangle in **Figure 5A** indicates the relocated epicentral distribution in the study area. The relocated earthquakes since 2009 are mainly distributed along the eastern branch of the Longquanshan fault zone and its eastern side, with most centered beneath Xinglong Town in Jintang County and Hongyuan Town in Jianyang County. The Hongyuan Town events occurred mainly in 2010. Seismicity in the Xinglong–Sanhe–Shisun area occurred mainly in 2009 and 2010, as well as after the 2013 Lushan earthquake. The influence of the 2008 M_S 8.0 Wenchuan and 2013 M_S 7.0 Lushan earthquakes on the seismicity of the Longquanshan fault zone is reflected in these observations. The aftershocks of the M_S 5.1 Qingbaijiang earthquake were ∼10 km southwest of the Xinglong earthquake cluster, and the epicenter of the M_S 5.1 mainshock was located between the eastern and western branches of the Longquanshan fault zone, ∼5 and 6 km from the eastern and western branches, respectively. The aftershock distribution strikes NE–SW, parallel to the Longquanshan fault zone, and is ∼6.0 km long and ∼2.5 km wide. The M_S 5.1 mainshock was located just north of the central part of the aftershock area (**Figure 5B**). Here we define 1 March 2020 as the boundary between the earlier and later aftershocks of the M_S 5.1 mainshock. The early aftershocks in February were generally smaller-magnitude events that were distributed to the southwest of the M_S 5.1 mainshock (red circles in **Figure 5B**), whereas the later aftershocks were relatively larger-magnitude events that were distributed to the east of the mainshock and included all of the relocated $M_L \geq 2.0$ earthquakes (green circles in **Figure 5B**).

We provide three depth profiles (A–A', B–B', and C–C' in **Figure 5A**) to further understand the seismogenic structure associated with the 2020 Qingbaijiang earthquake. These profiles focus on the M_S 5.1 Qingbaijiang earthquake sequence (B–B' and C–C' in **Figure 6**) and the earthquake clusters in the Xinglong–Sanhe–Shisun area (A–A' in **Figure 5C**).

Profile A–A' is perpendicular to the strike of the Longquanshan fault zone and intersects the main earthquake cluster in the Xinglong–Sanhe–Shisun area (**Figure 5A**). All of the relocated events within 5 km of the profile are plotted to discern the spatial distribution of the earthquake clusters. Three clusters are identified, which appear to form a parallel imbricate feature consisting of three steep NW-dipping faults

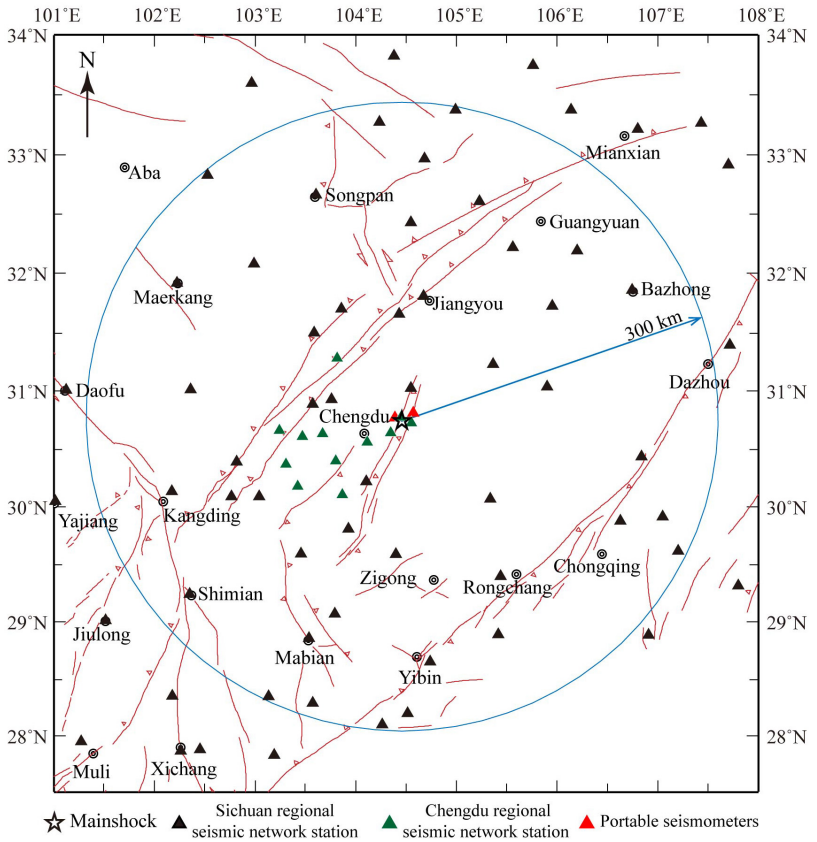

FIGURE 3 | Distribution of seismic stations (triangles) and known faults (red lines) around the epicenter of the M_S 5.1 Qingbaijiang earthquake (star). There were 55 broadband seismic stations (black and green triangles) and two portable SP seismometers (red triangles) within a 300 km epicentral distance of the mainshock.

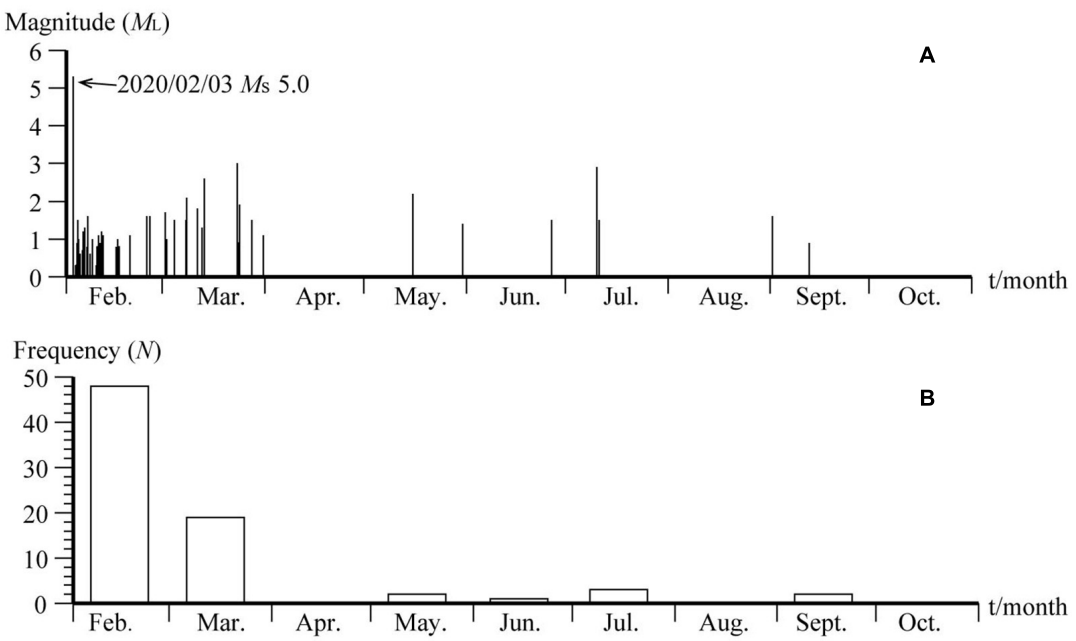

FIGURE 4 | *M–t* **(A)** and *N–t* **(B)** plots of the $M_L \geq 0.1$ events in the M_S 5.1 Qingbaijiang earthquake sequence during the 3 February–31 October 2020 period.

TABLE 1 | One-dimensional velocity model in the Longquanshan area.

Layer number	1	2	3	4	5	6	7	8	9	10	11	12
Top depth	0.0	6.0	8.0	10.0	16.0	18.0	20.0	25.0	28.0	34.0	43.0	61.0
Vp (km/s)	5.15	5.64	5.72	5.96	6.13	6.22	6.44	6.59	6.71	6.75	7.62	7.79

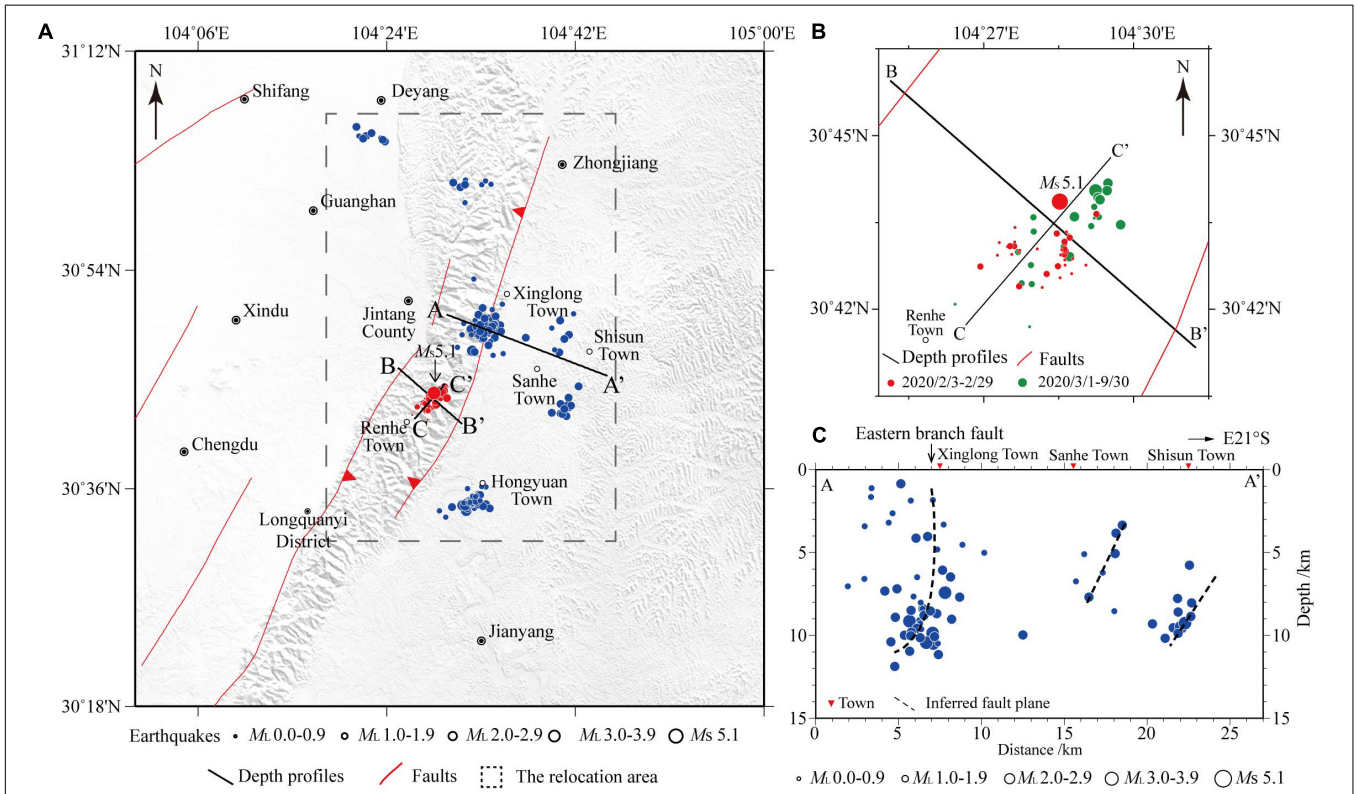

FIGURE 5 | Distribution of relocated epicenters. **(A)** Map of the relocated epicentral distribution across the central and northern segments of the Longquanshan fault zone since 2009; blue circles indicate the earthquakes since 2009, and red circles indicate the events in the 2020 M_S 5.1 Qingbaijiang earthquake sequence. **(B)** Map of the relocated epicentral distribution of the M_S 5.1 Qingbaijiang earthquake sequence. The aftershock distribution strikes NE–SW, with the M_S 5.1 mainshock located in the northern part of the aftershock area. **(C)** Depth distribution of relocated events along the A–A' profile. The three clusters appear to form a parallel imbricate feature consisting of three steep NW-dipping faults.

with focal depths concentrated in the upper 12 km of the crust. The two earthquake clusters along the eastern part of the profile are relatively small, distributed below Sanhe Town and Shisun Town, respectively, and not associated with surface ruptures. These two clusters occurred along planes dipping at ∼60° to the NW. The largest earthquake cluster near Xinglong Town has a "shovel-shaped" distribution that is nearly vertical in the uppermost crust and NW-dipping below 8 km depth. We suggest that the distribution of these earthquake clusters, which are located just below the surface expression of the eastern branch, reflects the geometry of this branch, which is consistent with regional geological and geophysical survey results (Huang and Tang, 1995).

Profiles B–B' and C–C' capture the short- and long-axis distributions of the M_S 5.1 Qingbaijiang earthquake aftershock area, respectively, showing all of the aftershocks that fall within 5 km of the profiles (**Figure 6**). The B–B' profile (**Figure 6A**) highlights a NW-dipping feature, with the aftershock distribution spanning depths of 3–6 km and the mainshock and most of the aftershocks being located above 5 km depth. The larger aftershocks ($M_L \geq 2.0$) were deeper than the smaller aftershocks. Beneath the Longquanshan anticline there is a decollement layer in the upper crust at 6–9 km depth (Hubbard et al., 2010; Jia et al., 2010; Li et al., 2015). It can therefore be inferred that the M_S 5.1 Qingbaijiang earthquake and its aftershocks occurred above this shallow detachment surface in the upper crust. The lack of aftershocks near the surface may indicate that the rupture did not extend to the surface. The distribution of the entire sequence in this section indicates that the M_S 5.1 Qingbaijiang earthquake occurred along a seismogenic fault plane dipping 56° to the NW, which is consistent with the dip direction of the eastern branch. If we extend this fault plane to the surface, it appears to meet the eastern branch fault. Therefore, we can infer that the M_S 5.1 Qingbaijiang earthquake ruptured the eastern branch of the Longquanshan fault zone at 3–6 km depth. The C–C' profile (**Figure 6B**) shows a northward deepening

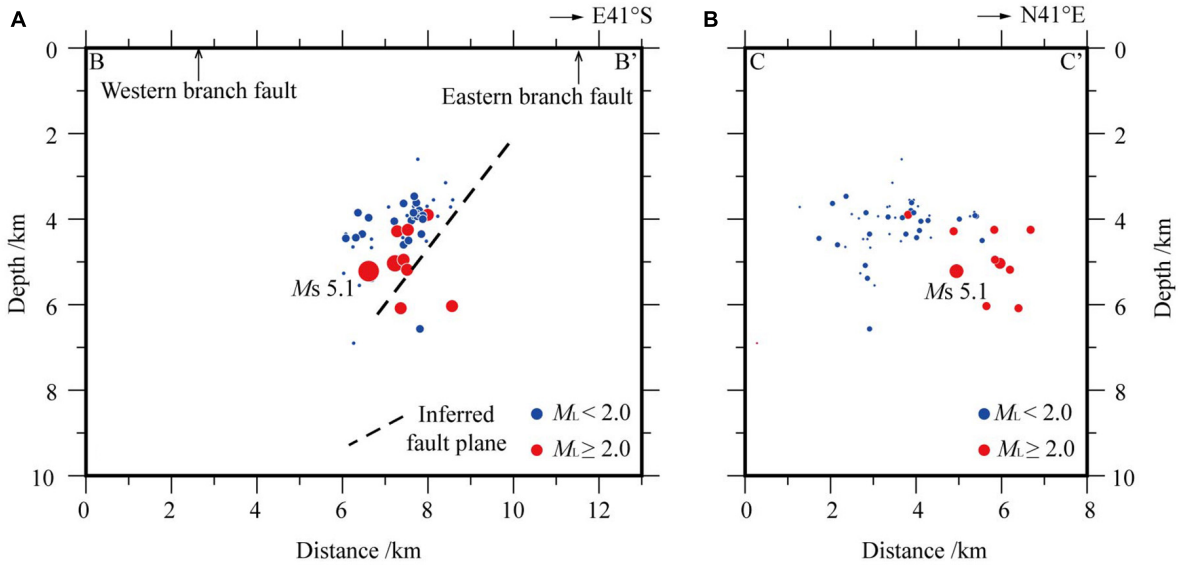

FIGURE 6 | Vertical cross-sections of the M_S 5.1 Qingbaijiang earthquake sequence. **(A)** Cross-section B–B', along the short axis of the M_S 5.1 sequence. This profile highlights a NW-dipping feature that appears to meet the eastern branch fault if it is extended to the surface. **(B)** Cross-section C–C', along the long axis of the M_S 5.1 sequence. This profile shows a northward deepening of the earthquake sequence, with smaller aftershocks in the southern part and larger aftershocks in the northern part.

of the earthquake sequence, with smaller aftershocks in the southern section that are concentrated at ∼4 km depth and larger aftershocks in the northern section that are all below 4 km depth, indicating segmentation along the eastern branch of the Longquanshan fault zone.

FOCAL MECHANISM INVERSION

Seismic Data and Focal Mechanism Solution Method

The focal mechanism solution, centroid depth, and moment magnitude of the M_S 5.1 Qingbaijiang earthquake were determined via the cut-and-paste (CAP) waveform inversion method (Zhao and Helmberger, 1994; Zhu and Helmberger, 1996). We chose the CAP method over other inversion methods since it needs fewer stations, and the inversion results are insensitive to lateral variations in the crust and less dependent on the velocity model (Tan et al., 2006; Zheng et al., 2009; Long et al., 2010; Yi et al., 2012; Luo et al., 2015). The CAP method can also constrain the focal depth using the surface wave amplitudes in the waveforms, thereby yielding a reliable focal centroid depth (Luo et al., 2015).

To calculate the focal mechanism of the mainshock, we analyzed the waveform records of permanent broadband seismic stations of the Sichuan Regional Seismological Network within a 50–300 km epicentral distance of the mainshock. We employed the frequency–wavenumber method (Zhu and Helmberger, 1996) to calculate Green's function using both a local 1-D velocity model (**Table 1**) and the model of Yi et al. (2020). We set a 2 s duration for the source time, 30 and 60 s waveform window lengths, and 0.05–0.20 Hz and 0.05–0.10 Hz band pass filters for the body waves and surface waves, respectively, in the CAP inversion. The inversion was conducted in 5° and 1 km increments to constrain the fault plane parameters and depth of the earthquake, respectively.

The obtained focal mechanism solution, centroid depth, and moment magnitude for the M_S 5.1 Qingbaijiang earthquake are shown in **Table 2**. The results for the two different velocity models are similar (**Table 2**); we selected the result based on the velocity model in **Table 1** as the focal mechanism solution for the event. The best fit to the waveforms was obtained at a 4 km centroid depth (**Figure 7**), with > 70% of the waveform components yielding correlation coefficients of > 93% (**Figure 8**).

The 4 km centroid depth of the M_S 5.1 mainshock is close to the relocated 5.2 km initial rupture depth, both of which indicate that the M_S 5.1 event occurred above the shallow detachment layer in the upper crust. The parameters of the focal mechanism solution (strike/dip/rake) are 22°/36°/91° for nodal plane I and 200°/54°/89° for nodal plane II, which indicate a thrust earthquake with a NE–SW rupture direction.

ANALYSIS OF THE SEISMOGENIC FAULT OF THE M_S 5.1 QINGBAIJIANG EARTHQUAKE AND IMPLICATIONS FOR SEISMIC HAZARD

Our preliminary analysis indicates that the seismogenic fault of the M_S 5.1 Qingbaijiang earthquake is along the eastern branch of the Longquanshan fault zone, with the coseismic rupture plane dipping 56° to the NW (nodal plane II). The initial rupture

TABLE 2 | Focal mechanism solutions for the M_S 5.1 Qingbaijiang earthquake from different velocity models.

Depth/km	Nodal plane I			Nodal plane II			*P* Axis		*T* Axis		*B* Axis		Magnitude		Velocity model
	strike/°	dip/°	rake/°	strike/°	dip/°	rake/°	azimuth/°	plunge/°	azimuth/°	plunge/°	azimuth/°	plunge/°	M_S	M_w	
4	22	36	91	200	54	89	291	9	105	81	201	1	5.1	4.61	**Table 1**
4	25	35	95	199	55	87	291	10	95	80	201	3		4.64	Yi et al. (2020)

depth obtained from the relocation analysis and the centroid depth obtained from waveform inversion suggest that this M_S 5.1 event was a moderate earthquake that occurred above the shallower detachment layer beneath the Longquanshan anticline. The sub-horizontal *P*-axis (azimuth of 291°) indicates that the tectonic stress field in the focal region is characterized by an subhorizontal principal compressive stress that trends WNW, which is consistent with the regional tectonic stress field in the South China Block (Heidbach et al., 2018; Wang and Shen, 2020). The earthquake depth, which is consistent with that of the destructive 1967 M_S 5.5 Renshou earthquake, may indicate that $M_S \geq 5.0$ destructive earthquakes along the Longquanshan fault zone have mainly occurred in the shallow part of the upper crust.

Since the 2008 Wenchuan earthquake, many studies have examined the seismic hazard of the Longquanshan fault zone. For example, Zhang et al. (2008) reported a ∼0.1 bar increase in the Coulomb stress of the Longquanshan fault zone after the Wenchuan earthquake. Qian and Han (2011) reported a 0.4–0.6 bar increase in stress along the northern segment of the Longquanshan fault zone after the Wenchuan earthquake, with this stress increase gradually decreasing from north to south along the fault zone, which is consistent with the observation that the seismicity along the fault zone was mainly clustered along the northern segment after the Wenchuan earthquake. Parsons et al. (2008) calculated the Coulomb stress change after the Wenchuan earthquake and suggested that the event increased both the stress state in the Sichuan Basin and the risk of earthquake occurrence. A comparative analysis of the seismicity before and after the 2008 Wenchuan earthquake found a significant increase in both the earthquake frequency and intensity in the Sichuan Basin (Yi et al., 2019). Moderate earthquakes occurred successively in the low-seismicity area of the Sichuan Basin, such as the 19 February 2013 M_S 4.7 Santai-Yanting earthquake, and the 29 July 2014 M_S 4.9 Zitong and M_S 4.6 Santai earthquakes, which could be related to stress loading in the Sichuan Basin due to the 2008 Wenchuan earthquake (Yi et al., 2019). However, Parsons et al. (2008) showed that the central and northern segments of the Longquanshan fault zone were in a negative zone of coseismic Coulomb stress disturbance due to the Wenchuan earthquake. Toda et al. (2008) reported a 0.1–0.3 bar stress reduction on a thrust fault to the south of Chengdu after the Wenchuan earthquake. Therefore, the influence of the 2008 Wenchuan earthquake on the seismicity and seismic hazard of the Longquanshan fault zone needs to be further investigated.

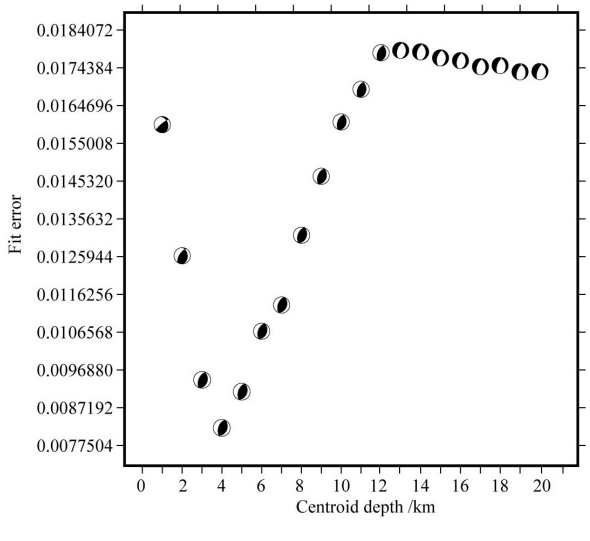

FIGURE 7 | Centroid depth variation in the residual error of the focal mechanism solution for the M_S 5.1 Qingbaijiang earthquake.

Previous studies have considered the western branch of the Longquanshan fault zone to be the main fault of the entire anticline (Deng et al., 1994; Huang and Tang, 1995; Tang et al., 1996; Wang et al., 2008; Wang and Lin, 2017), leading to the conclusion that the western branch represents a greater seismic hazard (Huang and Tang, 1995; Zhang et al., 2020). Luo et al. (2008) believe that the Longquanshan anticline formed under E–W compression related to collision between the Qinghai-Tibet Plateau and South China Block, which formed an anti-thrust pattern along the front of the Longmenshan thrust belt. The Longquanshan anticline is a shallow structure that has formed via multi-stage subduction and subsequent emplacement of deep material from the South China Block to the deeper sections of the LFTB and the West Sichuan Plateau. The eastern branch is a back-fault associated with the entire fold system, similar to the back-fault on the main fault plane of the 2013 M_S 7.0 Lushan earthquake (Long et al., 2015). However, another possibility is that the Longquanshan fault zone and LFTB are components of the same structural system, such that the Longquanshan fault zone forms the southeastern boundary of the LFTB nappe foreland basin in western Sichuan (Chen et al., 1994; Zhang et al., 2003; Liu, 2007). The eastern branch of the Longquanshan fault zone would be considered the main fault in this combined structural system, whereas the western branch would be a back-fault associated with the entire fold system. Most earthquakes, including the M_S 5.1 Qingbaijiang earthquake sequence, have occurred along the eastern branch since 2009, supporting this latter structural model. Further investigations of the dynamic

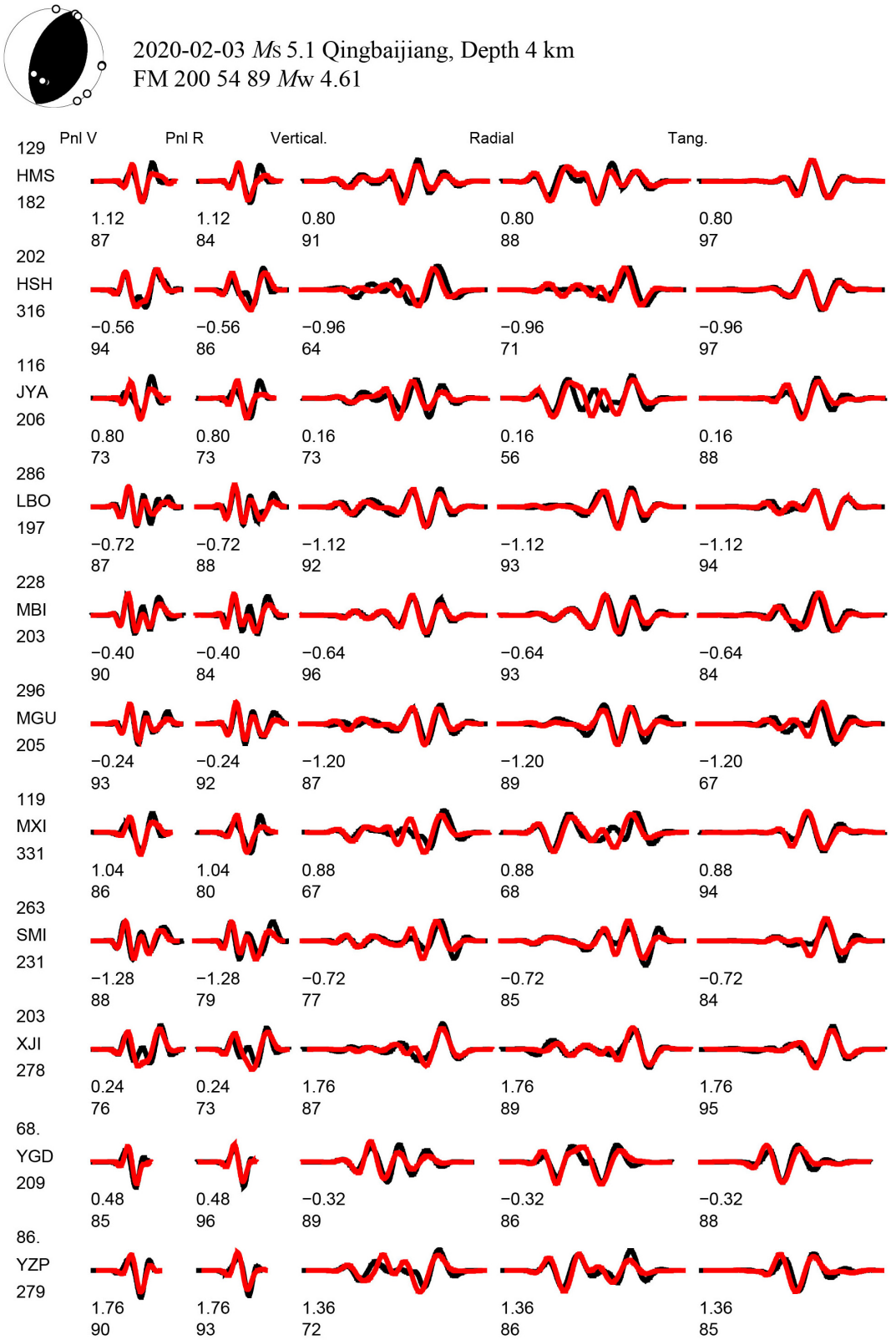

FIGURE 8 | Comparison of synthetic (red) and observed (black) waveforms at the best fitting depth for the M_S 5.1 Qingbaijiang earthquake. The relative time shift (in s; upper) and correlation coefficient (in%; lower) are provided below each trace. The station names are given to the left, with the epicentral distance (in km; upper) and azimuth (in degree; lower) provided.

origin, tectonic setting, and seismic hazard of the Longquanshan fault zone need to be undertaken to resolve these discrepancies.

CONCLUSION

We analyzed seismic phase and waveform data recorded by the Sichuan and Chengdu regional seismic networks to relocate the earthquakes that have occurred along the central and northern segments of the Longquanshan fault zone since 2009, including the M_S 5.1 Qingbaijiang earthquake sequence, using the multi-stage method. We also calculated the focal mechanism of the M_S 5.1 mainshock using the CAP waveform inversion method.

The M_S 5.1 Qingbaijiang earthquake occurred along a NE–SW-striking fault, consistent with the trend of the Longquanshan fault zone, at an initial rupture depth of 5.2 km. The earthquake clusters that have occurred along the Longquanshan fault zone since 2009, including the M_S 5.1 Qingbaijiang earthquake sequence, were located along NW-dipping features that formed a parallel imbricate pattern, which is identical to the fault geometry along the eastern branch of the Longquanshan fault zone. The mainshock had a centroid depth of 4 km and a thrust-type focal mechanism along a NW-dipping fault plane, similar to the structure of the eastern branch. Therefore, the M_S 5.1 Qingbaijiang earthquake was a pure thrusting event along the eastern branch of the Longquanshan fault zone, and nodal plane II of the focal mechanism solution represents the coseismic rupture plane. We conclude that the M_S 5.1 Qingbaijiang earthquake was a moderate earthquake above the shallow detachment layer beneath the Longquanshan Anticline and was controlled by the regional tectonic stress field, as inferred from regional geological constraints.

The focal depth of the M_S 5.1 Qingbaijiang earthquake, which is consistent with that of the 1967 M_S 5.5 Renshou earthquake, may indicate that the destructive $M_S \geq 5.0$ earthquakes along the Longquanshan fault zone occur primarily in the shallow part of the upper crust. Our study provides valuable data for future studies on the seismogenesis and seismic hazard of the Longquanshan fault zone.

AUTHOR'S NOTE

MZ, Master, engineer, mainly engaged in seismic activity research.

DATA AVAILABILITY STATEMENT

The original contributions presented in the study are included in the article, further inquiries can be directed to the corresponding author.

AUTHOR CONTRIBUTIONS

MZ mainly completed the writing of the manuscript. FL mainly completed the data processing and supported the completion of the manuscript. GY mainly formed the idea of the manuscript and supported the completion of the manuscript. ML, JX, and SW participated worked for the manuscript. All authors contributed to the article and approved the submitted version.

FUNDING

The research was supported by the National Science Foundation of China (41574047) and the National Key R&D Program of China (2018YFC150330501 and 2020YFA0710603-01).

ACKNOWLEDGMENTS

We are grateful to Prof. Zhu Lupei of San Luis University of the United States for providing the CAP program, and to the reviewers for valuable suggestions. GMT software was used to plot a part of the figures. We are very grateful to the editors and reviewers for their constructive comments and thoughtful suggestions.

REFERENCES

Burchfiel, B. C. (2004). New technology, new geological challenges. *GSA Today* 14, 4–10. doi: 10.1130/1052-51732004014<4:panngc<2.0.co;2

Burchfiel, B. C., Chen, Z. L., Liu Yupinc, L., and Royden. (1995). Tectonics of the Longmen Shan and Adjacent Regions, Central China. *Int. Geol. Rev.* 37, 661–735. doi: 10.1080/00206819509465424

Burchfiel, B. C., Royden, L. H., vander Hilst, R. D., Hager, B. H., Chen, Z., King, R. W., et al. (2008). A geological and geophysical context for the Wenchuan earthquake of 12 May 2008, Sichuan, People's Republic of China. *GSA Today* 18, 4–11. doi: 10.1130/gsatg18a.1

Chen, S. F., and Wilson, C. J. L. (1996). Emplacement of the Longmen Shan Thrust-Nappe Belt along the eastern margin of the Tibetan Plateau. *J. Struct. Geol.* 18, 413–430. doi: 10.1016/0191-8141(95)00096-V

Chen, S. F., Wilson, C., Deng, Q. D., Zhao, X. L., and Zhi, L. L. (1994). Active faulting and block movement associated with large earthquakes in the Min Shan and Longmen Mountains,northeastern Tibetan plateau. *J. Geophys. Res.* 99, 20–25. doi: 10.1029/94JB02132

Cheng, E. L. (1981). Recent tectonic stress field and tectonic movement of the Sichuan Province and its vicinity. *Acta Seismol. Sin.* 3, 231–241.

Deng, Q. D., Chen, S. F., and Zhao, X. L. (1994). Tectonics, scismisity and dynamics of Longmenshan mountains and its adjacent regions. *Seismol. Geol.* 16, 389–403.

Heidbach, O., Rajabi, M., Cui, X., Fuchs, K., Müller, B., Reinecker, J., et al. (2018). The World Stress Map database release 2016: Crustal stress pattern across scales. *Tectonophysics* 744, 484–498. doi: 10.1016/j.tecto.2018.07.007

Houseman, G., and England, P. (1986). Finite strain calculations of continental deformation: 1. Method and general results for convergent zones. *J. Geophys. Res. Solid Earth* 91, 3651–3663. doi: 10.1029/JB091iB03p03651

Huang, W., and Jiang, W. L. (2012). Discussion on the late quaternary activity and earthquake risk potential of Longquanshan Fault in Sichuan. *Northwestern Seismol. J.* 34, 50–56. doi: 10.3969/j.issn.1000-0844.2012.01.010

Huang, Z. Z., and Tang, R. C. (1995). The Longquanshan fault zone and exploration of potential earthquake ability. *Earthquake Res. Sichuan* 1, 18–23.

Hubbard, J., and Shaw, J. H. (2009). Uplift of the Longmen Shan and Tibetan plateau, and the 2008 Wenchuan (M=7.9) earthquake. *Nature* 458, 194–197. doi: 10.1038/nature07837

Hubbard, J., Shaw, J. H., and Klinger, Y. (2010). Structural Setting of the 2008 Mw 7.9 Wenchuan. China, Earthquake. *Bull. Seismol. Soc. Am.* 100, 2713–2735. doi: 10.1785/0120090341

Jia, D., Li, Y., Lin, A., Wang, M., Chen, W., Wu, X., et al. (2010). Structural model of 2008 Mw 7.9 Wenchuan earthquakes in the rejuvenated Longmen Shan thrust belt China. *Tectonophysics* 491, 174–184. doi: 10.1016/j.tecto.2009.08.040

Kirby, E., Reiners, P. W., Krol, M. A., Whipple, K. X., Hodges, K. V., Farley, K. A., et al. (2002). Late Cenozoic evolution of the eastern margin of the Tibetan Plateau: Inferences from 40Ar/39Ar and (U-Th)/He thermochronolgy. *Tectonics* 21:1001. doi: 10.1029/2000TC001246

Kirby, E., Whipple, K., and Harkins, N. (2008). Topography reveals seismic hazard. *Nat. Geosci.* 1, 485–487. doi: 10.1038/ngeo265

Kissling, E., Ellsworth, W., Eberhart-Phillips, D., and Kradolfer, U. (1994). Initial reference models in local earthquake tomography. *J. Geophys. Res. Solid Earth* 99, 19635–19646. doi: 10.1029/93JB03138

Kissling, E., Kradolfer, U., and Maurer, H. (1995). *VELEST user ES guide short introduction*. Zürich: ETH Zuerich.

Klein, F. W. (1989). HYPOINVERSE, a program for VAX computers to solve for earthquake locations and magnitudes. *U S. Geol. Survey Open File Rep.* 59, 89–314.

Li, K., Xu, X. W., and Tang, X. B. (2013). Using deformation terraces to confine the shortening and uplift of the Longquan anticline. *Seismol. Geol.* 35, 22–36. doi: 10.3969/j.issn.0253-4967.2013.01.002

Li, K., Xu, X. W., Tan, X. B., Chen, G. H., Xu, C., and Kang, W. J. (2015). Late Quaternary deformation of the Longquan anticline in the Longmenshan thrust belt, eastern Tibet, and its tectonic implication. *J. Asian Earth Sci.* 112, 1–10. doi: 10.1016/j.jseaes.2015.08.022

Li, Y. Q., Jia, D., Shaw, J. H., Hubbard, J., Lin, A. M., Wang, M. M., et al. (2010). Structural interpretation of the coseismic faults of the Wenchuan earthquake: three-dimensional modeling of the Longmen Shan fold-and-thrust belt. *J. Geophys. Res.* 115, 1–26. doi: 10.1029/2009JB006824

Li, Y., and Zeng, Y. F. (1994). On the sedimentary response to thrusting of Longmenshan trust belt in Chengdu Basin. *J. Mineral Petrol.* 14, 58–66.

Li, Z. G., Jia, D., and Chen, W. (2012). Structural geometry and deformation mechanism of the Longquan anticline in the Longmen Shan fold-and-thrust belt, eastern Tibet. *J. Asian Earth Sci.* 64, 223–234. doi: 10.1016/j.jseaes.2012.12.022

Liu, S. (2007). *Structural characteristics of the thrust fold of foreland – a case study of thrust fold at Micang and Longmen Mountains*. Ph.D. thesis. Beijing: Institute of Geology China Earthquake Administration.

Liu-Zeng, J., Zhang, Z., Wen, L., Tapponnier, P., Sun, J., Xing, X., et al. (2009). Co-seismic ruptures of the 12 May 2008, Ms 8.0 Wenchuan earthquake, Sichuan: East–west crustal shortening on oblique, parallel thrusts along the eastern edge of Tibet. *Earth Planetary Sci. Lett.* 286, 355–370. doi: 10.1016/j.epsl.2009.07.017

Long, F., Wen, X. Z., Ruan, X., Zhao, M., and Yi, G. X. (2015). A more accurate relocation of the 2013Ms7.0 Lushan, Sichuan, China, earthquake sequence, and the seismogenic structure analysis. *J. Seismol.* 19, 653–665. doi: 10.1007/s10950-015-9485-0

Long, F., Zhang, Y. J., Wen, X. Z., and Ni, S. D. (2010). Focal mechanism solution of $M_L \geq 4.0$ events in the MS6.1 Panzhihua-Huili earthquake sequence of Aug 30, 2008. *Chin. J. Geophys.* 53, 2852–2860.

Luo, Y., Zhao, L., Zeng, X. F., and Gao, Y. (2015). Focal mechanisms of the Lushan earthquake sequence and spatial variation of the stress field. *Sci. China Earth Sci.* 58, 1148–1158. doi: 10.1007/s11430-014-5017-y

Luo, Z. L., Yong, Z. Q., Liu, S. G., Sun, W., Deng, B., Yang, R. J., et al. (2008). Relationship between C-subduction and the Wenchuan earthquake and suggestions on preventing earthquakes and mitigationg disaters. *J. Chengdu Univers. Technol.* 35, 337–347. doi: 10.3969/j.issn.1671-9727.2008.04.001

Lv, J., Wang, X. S., Su, J. R., Pan, L. S., Li, Z., Yin, L. W., et al. (2013). Hypocentral location and source mechanism of the MS7.0 Lushan earthquake sequence. *Chin. J. Geophys.* 56, 1753–1763. doi: 10.6038/cjg20130533

Michael, A. J. (1988). Effects of three-dimensional velocity structure on the seismicity of the 1984 Morgan Hill, California, aftershock sequence. *Bull. Seismol. Soc. Am.* 78, 1199–1221.

Molnar, P. H., and Tapponnier, P. (1975). Cenozoic tectonics of Asia: Effects of a continental collision. *Science* 189, 419–426. doi: 10.1126/science.189.4201.419

Parsons, T., Ji, C., and Kirby, E. (2008). Stress changes from the 2008 Wenchuan earthquake and increased hazard in the Sichuan Basin. *Nature* 454, 509–510. doi: 10.1038/nature07177

Presti, D., Orecchio, B., Falcone, G., and Neri, G. (2008). Linear versus nonlinear earthquake location and seismogenic fault detection in the southern Tyrrhenian Sea. Italy. *Geophys. J. Int.* 172, 607–618. doi: 10.1111/j.1365-246x.2007.03642.x

Qian, Q., and Han, Z. J. (2011). The research in the change of the earthquake occurrence probability in Longquan Shan fault after the Wenchuan earthquake. *Prog. Geophys.* 26, 489–497. doi: 10.3969/j.issn.1004-2903.2011.02.013

Shearer, P. (1997). Improving local earthquake locations using the L1 norm and waveform cross correlation: application to the Whittier Narrows, California, aftershock sequence. *J. Geophys. Res. Solid Earth* 102, 8269–8283. doi: 10.1029/96JB03228

Tan, Y., Zhu, L. P., Helmberger, D. V., and Saikia, C. K. (2006). Locating and modeling regional earthquakes with two stations. *J. Geophys. Res.* 111:B11. doi: 10.1029/2005JB003775

Tang, R. C., Huang, Z. Z., Qian, H., Gong, Y., Wen, D. H., Ma, S. H., et al. (1996). Main features and potential seismic capability of active fault belts in Chengdu Depression. *Earthquake Res. China* 3, 285–293.

Tapponnier, P., and Molnar, P. (1977). Active faulting and tectonics in China. *J. Geophys. Res.* 82, 2905–2930. doi: 10.1029/JB082i020p02905

Tapponnier, P., Peltzer, G., Le Dain, A. Y., Armijo, R., and Cobbold, P. (1982). Propagating extrusion tectonics in Asia: new insights from simple experiments with plasticine. *Geology* 10, 611–616.

Tapponnier, P., Xu, Z., Roger, F., Meyer, B., Arnaud, N., Wittlinger, G., et al. (2001). Oblique stepwise rise and growth of the Tibet Plateau. *Science* 294, 1671–1677. doi: 10.1126/science.105978

Toda, S., Lin, J., Meghraoui, M., and Stein, R. S. (2008). 12 May 2008 M = 7.9 Wenchuan, China, earthquake calculated to increase failure stress and seismicity rate on three major fault systems. *Geophys. Res. Lett.* 35, L17305–L17301. doi: 10.1029/2008GL034903

Waldhauser, F., and Ellsworth, W. L. (2000). A double-difference earthquake location algorithm: method and application to the northern Hayward fault, California. *Bull. Seismol. Soc. Am.* 90, 1353–1368.

Wang, E., Kirby, E., Furlong, K. P., van Soest, M., Xu, G., Shi, X., et al. (2012). Two-phase growth of high topography in eastern Tibet during the Cenozoic. *Nat. Geosci.* 5:640. doi: 10.1038/ngeo1538

Wang, H., Ran, Y., Chen, L., Shi, X., Liu, R., and Gomez, F. (2010). Determination of horizontal shortening and amount of reverse-faulting from trenching across the surface rupture of the 2008 M W 7.9 Wenchuan earthquake, China. *Tectonophysics* 491, 10–20. doi: 10.1016/j.tecto.2010.03.019

Wang, M., and Lin, A. (2017). Active thrusting of the Longquan Fault in the central Sichuan basin, China, and the seismotectonic behavior in the Longmen Shan fold-and-thrust belt. *J. Geophys. Res. Solid Earth* 122, 5639–5662. doi: 10.1002/2016JB013391

Wang, M., and Shen, Z. (2020). Present-Day Crustal Deformation of Continental China Derived From GPS and Its Tectonic Implications. *J. Geophys. Res. Solid Earth* 125:2019JB018774. doi: 10.1029/2019JB018774

Wang, Q., Qiao, X., Lan, Q., Freymueller, J., Yang, S., Xu, C., et al. (2011). Rupture of deep faults in the 2008 Wenchuan earthquake and uplift of the Longmen Shan. *Nat. Geosci.* 4, 634–640. doi: 10.1038/ngeo1210

Wang, W. T., Jia, D., Li, C. Y., Zheng, W. J., and Wei, Z. Y. (2008). Preliminary investigation on deformation characteristics and activity of Longquanshan fault belt in Sichuan. *Seismol. Geol.* 30, 968–979.

Wiemer, S., and Wyss, M. (2000). Minimum magnitude of completeness in earthquake catalogs: examples from Alaska, the Western United States, and Japan. *Bull. Seismol. Soc. Am.* 90, 859–869. doi: 10.1785/0119990114

Xu, S. S., Ren, H., and Song, J. (2006). Primary study on the seismicity along the faults of Longquanshan. *Earthquake Res. Sichuan* 2, 21–27. doi: 10.3969/j.issn.1001-8115.2006.02.005

Xu, X. W., Wen, X. Z., Chen, G. H., Li, C. Y., Zheng, W. J., Zhnag, S. M., et al. (2013). Lushan M S 7.0 earthquake: A blind reserve-fault event. *Chin. Sci. Bull.* 58, 3437–3443. doi: 10.1007/s11434-013-5999-4

Xu, X. W., Wen, X. Z., Guihua, Y., Chen, G., Klinger, Y., Hubbard, J., et al. (2009). Coseismic reverse- and oblique-slip surface faulting generated by the 2008 Mw 7.9 Wenchuan earthquake, China. *Geology* 37, 515–518. doi: 10.1130/G25462A.1

Yi, G. X., Long, F., and Zhang, Z. W. (2012). Spatial and temporal variation of focal mechanisms for aftershocks of the 2008 MS8.0 Wenchuan earthquake. *Chin. J. Geophys.* 55, 1213–1227. doi: 10.6038/j.issn.0001-5733.2012.04.017

Yi, G. X., Long, F., Liang, M. J., Zhang, H. P., Zhao, M., Ye, Y. Q., et al. (2017). Focal mechanism solutions and seismogenic structure of the 8 August 2018 M7.0 Jiuzhaigou earthquake and its aftershocks, northern Sichuan. *Chin. J. Geophys.* 60, 4083–4097. doi: 10.6038/cjg20171033

Yi, G. X., Long, F., Liang, M. J., Zhao, M., and Wang, S. W. (2020). Geometry and tectonic deformation of seismogenic structures in the Rongxian-Weiyuan-Zizhong region, Sichuan Basin: insights from mechanism solutions. *Chin. J. Geophys.* 63, 3275–3291.

Yi, G. X., Long, F., Liang, M. J., Zhao, M., Wang, S. W., Gong, Y., et al. (2019). Focal mechanism solutions and seismogenic structure of the 17 June 2019 MS6.0 Sichuan Changning earthquake sequence. *Chin. J. Geophys.* 62, 3432–3447. doi: 10.6038/cjg2019N0297

Yi, G. X., Long, F., Wen, X. Z., Liang, M. J., and Wang, S. W. (2015). Seismogenic structure of the M6.3 Kangding earthquake sequence on 22 Nov. Southwestern China. *Chin. J. Geophys.* 58, 1205–1219. doi: 10.6038/cjg20150410

Yin, A. (2010). A special issue on the great 12 May 2008 Wenchuan earthquake (*M*w 7.9): Observations and unanswered questions. *Tectonophysics* 491, 1–9. doi: 10.1016/j.tecto.2010.05.019

Yin, A., and Harrison, T. M. (2000). Geologic Evolution of the Himalayan-Tibetan Orogen. *Annu. Rev. Earth Planetary Sci.* 28, 211–280. doi: 10.1146/annurev.earth.28.1.211

Zhang, G. H., Shan, X. J., and Li, W. D. (2008). The coulomb failure stress change associated with th MS8.0 Wenchuan earthquake and the risk prediction of its surrounding faults. *Seismol. Geol.* 30, 935–944. doi: 10.3969/j.issn.0253-4967.2008.04.010

Zhang, P. Z. (2013). A review on active tectonics and deep crustal processes of the Western Sichuan region, eastern margin of the Tibetan Plateau. *Tectonophysics* 584, 7–22. doi: 10.1016/j.tecto.2012.02.021

Zhang, P. Z., Wen, X. Z., Shen, Z. K., and Chen, J. H. (2010). Oblique, High-Angle, Listric-Reverse Faulting and Associated Development of Strain: TheWenchuan Earthquake of May 12, 2008, Sichuan, China. *Annu. Rev. Earth Planet. Sci.* 38, 353–382. doi: 10.1146/annurev-earth-040809-152602

Zhang, W., Zhou, R., He, Y., Liu, S., Ma, and Chao. (2020). Characteristic of Shallow Structure and Fault Activity in Western Piedmont to Longquanshan. *J. Geodesy Geodynam.* 40, 942–946. doi: 10.14075/j.jgg.2020.09.013

Zhang, Y. Q., Yang, N., Chen, W., Ma, Y. S., and Meng, H. (2003). Late Cenozoic tectonic deformation history of the east-west geomorphological boundary zone of china and uplift process of the eastern margin of the Tibetan Plateau. *Earth Sci. Front.* 10, 599–612. doi: 10.3321/j.issn:1005-2321.2003.04.026

Zhao, L. S., and Helmberger, D. V. (1994). Source estimation from broadband regional seismograms. *Bull. Seismol. Soc. Am.* 84, 91–104. doi: 10.1029/93JB02965

Zhao, Z., and Zhang, R. S. (1987). Primary study of crustal and upper mantle velocity structure of Sichuan Province. *Acta Seismol. Sin.* 1987, 44–56.

Zheng, Y., Ma, H. S., Lv, J., Ni, S. D., Li, Y. C., and Wei, S. J. (2009). The focal mechanism solution of Wenchuan Earthquake strong aftershock (MS=5.6) and its relationship with seismogenic structure. *Sci. China* 39, 413–426. doi: 10.1360/zd2009-39-4-413

Zhu, L. P., and Helmberger, D. V. (1996). Advancement in source estimation techniques using broadband regional seismograms. *Bull. Seismol. Soc. Am.* 86, 1634–1641. doi: 10.1029/96JB02296

Conflict of Interest: The authors declare that the research was conducted in the absence of any commercial or financial relationships that could be construed as a potential conflict of interest.